A new method for automatic calibration of 5-port reflectometers

*Fernando Rangel de Sousa, *Bernard Huyart and †Robson N. de Lima
*COMELEC - GET TELECOM Paris. 46 rue Barrault, 75634 Paris - FR
Tel.:+33(0)145-81-7208, Fax:+33(0)145-80-4036
e-mail:fernando.rangel@enst.fr,bernard.huyart@enst.fr
† DEE/EP - UFBA. Rua Aristides Novis, 2, Federação, Salvador - BA, BR
e-mail: delima@ufba.br

Abstract

The five-port reflectometer has been recently applied to demodulators and radars, offering an alternative to classic In-Phase/Quadrature (I/Q) discriminators. In these applications, calibration of the reflectometer is an important task. Most of the methods developed are suitable for the instrumentation and measurement field and present a high degree of complexity. We propose in this paper a new method for calibrating six or five-port reflectometers. This procedure is advantageous for its simplicity and is particularly useful for calibration in manufacturing processes.

I. INTRODUCTION

The six-port technique was introduced in the Seventies as an alternative network analyser [1]. This technique was particularly interesting thanks to the use of power detectors instead of mixers which provided simpler circuits in comparison with its heterodyne counterpart. When the need of low-cost RF receivers arised, the six-port experts proposed demodulators based on the principle of the six-port network analyser [2].

In Zero-IF demodulators, a vector decomposition in an orthogonal base is performed in the incoming RF signal. The base generator circuits must be carefully designed to avoid imbalance and consequently to avoid BER degradation [3]. Some authors proposed six-port receivers preserving the orthogonal base principle and used analog circuits to calculate the I/Q baseband signals from the reflectometer outupt powers [2], [4]. The same Zero-IF design constraints are applicable here since there is no calibration procedure. Other researchers followed the former network analyser approach, where the I and Q components are digitally determined [5], [6]. In this case, the design of the vector base circuits is less restrictive, the base is non-orthogonal and its parameters are found by calibration. The five-port Zero-IF principle has also been applied to radars [7] and PLLs [8].

Calibration is the most important task when dealing with six or five-port systems. It is necessary to allow the determination of I and Q values from power measurements. Many works describing calibration procedures have been proposed along the years [9]–[11]. Some of them were developed for microwave instrumentation and measurement applications and are rather complex [9]. Some others are more adequate to modern systems like direct conversion receivers [11]. In [10] a calibration method based on artificial neural networks was proposed. This technique is advantageous for permitting automatic procedures, nevertheless it requires a great amount of time to be accomplished and demands a large number of known standards necessary to the network trainning. An adaptative technique is presented in [11]. It is based on the training sequences commonly available in wireless transmissions and provides for self-adaptation. The drawback encountered in this proposal is its restriction to weak RF signals (inferior to -20 dBm as reported by the author).

 ISSN 1516-7399

We propose in this paper a new calibration method for five-port reflectometer based systems which is valid for any level of incoming RF signal and can be extended to six-port reflectometers as well. It is based on analytical description of the system behavior and measurements performed when two signals with a slight frequency difference are connected to the reflectometer's inputs. The simplicity of the method provides for automatic calibration of modern applications like wireless receivers and is specially suitable for being used during manufacturing process. The method was validated using data obtained from simulations and measurements.

II. The Five Port Reflectometer Equations

A system based on a five-port reflectometer may be represented by the block diagram of Figure 1. It consists of an interferometric junction with two inputs (1, 2) and three outputs (3, 4, 5), three diode power detectors (d_1, d_2, d_3), three analog-to-digital converters and a digital signal processor (DSP). This system generates a signal $\rho(n)$ in the digital domain representing the complex ratio between the two input signals $v_{rf}(t)$ and $v_{LO}(t)$, where $v_{rf}(t) = Re\{V_{RF}(t)e^{j(\omega t+\theta(t))}\}$ and $v_{LO}(t) = V_{LO}\cos\omega t$.

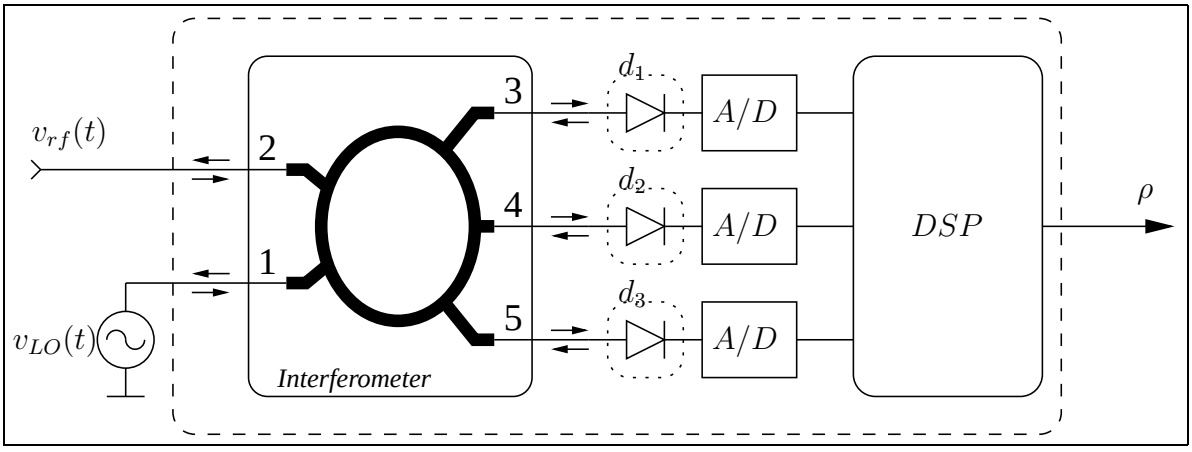

Fig. 1. System based on a five port reflectometer suitable to determine $\rho = \frac{a_2}{a_1}$

The reflectometer performs a vectorial addition of the two RF signals connected at its inputs under various phases. Then, the outcoming RF signals at the reflectometer ports 3, 4 and 5 have the form:

$$v_{rfi}(t) = \sqrt{a_i}V_{LO}\cos(\omega t + \gamma_i) + \sqrt{b_i}V_{RF}(t)\cos(\omega t + \theta(t) + \lambda_i) \quad (1)$$

where $i = 3\cdots5$, a_i and b_i depend on the circuit characteristics, γ_i is the phase of $v_{LO}(t)$ at port i with respect to port 1 and λ_i is the phase of $v_{rf}(t)$ at port i relative to port 2 . The power dectectors connected at ports 3, 4 and 5 comprise schottky diodes and RC low-pass filters as shown in Figure 2. The exponential law which relates the current i_D through and the voltage v_D between the terminals of a diode has a predominant second order behavior when $v_D << V_T$ ($V_T \approx 25\ mV$). Then, the voltage values measured at the power detectors' outputs are given by the following equation:

$$v_i(t) = a_iV_{LO}^2 + b_iV_{RF}^2(t) + c_iV_{RF}(t)\cos(\theta(t) - \phi_i) \quad (2)$$

where $i = 3\cdots5$, $\phi_i = \gamma_i - \lambda_i$; c_i depends on a_i, b_i and V_{LO} which is supposed to be constant. The third term of (2) may be understood as a projection of $v_{rf}(t)$ over a base composed by vectors of the form: $c_ie^{j\phi_i}$. When the condition $v_D << V_T$ can not be assured, we apply a curve fitting procedure to extend the validity of (2) [12].

 ISSN 1516-7399

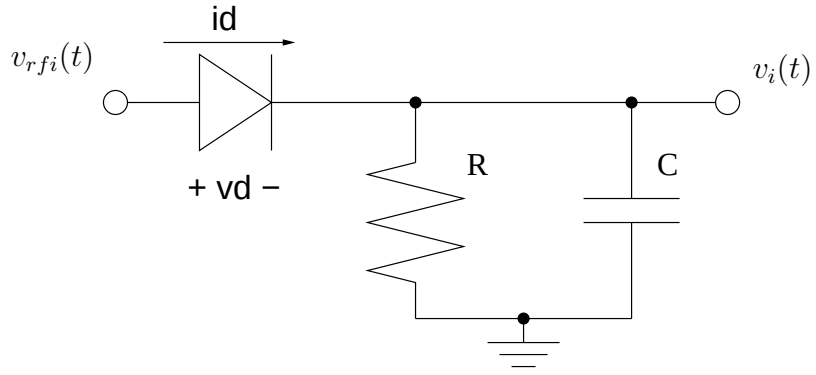

Fig. 2. Power detector

After some trigonometric manipulations, (2) becomes the expression below:

$$\hat{v_i}(t) = b_i V_{RF}^2(t) + c_i \cos\phi_i U(t) + c_i \sin\phi_i V(t) \tag{3}$$

where $i = 3 \cdots 5$, $\hat{v_i}(t) = v_i(t) - a_i V_{LO}^2$ and $U(t) = V_{RF}(t)\cos\theta(t)$ and $V(t) = V_{RF}(t)\sin\theta(t)$ are respectively the real and the imaginary part of the complex envelope of $v_{rf}(t)$.

The linear system formed by (3) can be solved for $U(t)$, $V(t)$ and $V_{RF}^2(t)$ as function of the measured voltages $\hat{v_i}(t)$. We are particularly interested in $U(t)$ and $V(t)$ which can be calculated from the following expressions:

$$U(t) = \hat{v_1}(t)x_1 + \hat{v_2}(t)x_2 + \hat{v_3}(t)x_3 \tag{4}$$

$$V(t) = \hat{v_1}(t)y_1 + \hat{v_2}(t)y_2 + \hat{v_3}(t)y_3 \tag{5}$$

where:

$$x_1 = \frac{1}{c_1 T}\left[\frac{b_2 c_3}{b_1 c_1}\sin\phi_3 - \frac{b_3 c_2}{b_1 c_1}\sin\phi_2\right] \tag{6}$$

$$x_2 = \frac{1}{c_1 T}\left[\frac{b_3}{b_1}\sin\phi_1 - \frac{c_3}{c_1}\sin\phi_3\right] \tag{7}$$

$$x_3 = \frac{1}{c_1 T}\left[\frac{c_2}{c_1}\sin\phi_2 - \frac{b_2}{b_1}\sin\phi_1\right] \tag{8}$$

$$y_1 = \frac{1}{c_1 T}\left[\frac{b_3 c_2}{b_1 c_1}\cos\phi_2 - \frac{b_2 c_3}{b_1 c_1}\cos\phi_3\right] \tag{9}$$

$$y_2 = \frac{1}{c_1 T}\left[\frac{c_3}{c_1}\cos\phi_3 - \frac{b_3}{b_1}\cos\phi_1\right] \tag{10}$$

$$y_3 = \frac{1}{c_1 T}\left[\frac{b_2}{b_1}\cos\phi_1 - \frac{c_2}{c_1}\cos\phi_2\right] \tag{11}$$

where:

$$T = \frac{b_3 c_2}{b_1 c_1}\sin(\phi_1 - \phi_2) + \frac{b_2 c_3}{b_1 c_1}\sin(\phi_3 - \phi_1) + \frac{c_2 c_3}{c_1^2}\sin(\phi_2 - \phi_3) \tag{12}$$

The calibration of the five-port system consists in finding x_i and y_i. In the next section we present a method which allows the determination of ϕ_1, ϕ_2, ϕ_3, c_1, b_2/b_1, b_3/b_1, c_2/c_1 and c_3/c_1.

 ISSN 1516-7399

III. THE CALIBRATION METHOD PROPOSED

Before describing how the constants are obtained, some simplifications should be done. First, we define $\phi_i' = \phi_i - \phi_0$ and choose $\phi_1' = 0$ which leads to $\phi_0 = \phi_1$. Then we replace ϕ_i by ϕ_i' in (2). This phase shift in $v_{RF}(t)$ allows the definition of $U'(t) = V_{RF}(t)\cos(\theta(t)+\phi_0)$ and $V'(t) = V_{RF}(t)\sin(\theta(t)+\phi_0)$. The relationship between $U(t)$, $V(t)$ and $U'(t)$, $V'(t)$ is expressed by:

$$U(t) = U'(t)\cos\phi_0 + V'(t)\sin\phi_0 \tag{13}$$

$$V(t) = V'(t)\cos\phi_0 - U'(t)\sin\phi_0 \tag{14}$$

The calibration procedure relies on the observation of the voltage values sampled at the three power detector outputs when $V_{RF}(n) = V_{RF}$ and $\theta(n) = n\Delta f$ in the discrete time version of (2). Δf is a frequency offset with respect to the LO frequency, $n = 0 \cdots N$, $N = 2\pi f_s/\Delta f$ and f_s is the sampling frequency. The waveforms of the sampled voltages have the form shown in Figure 3.

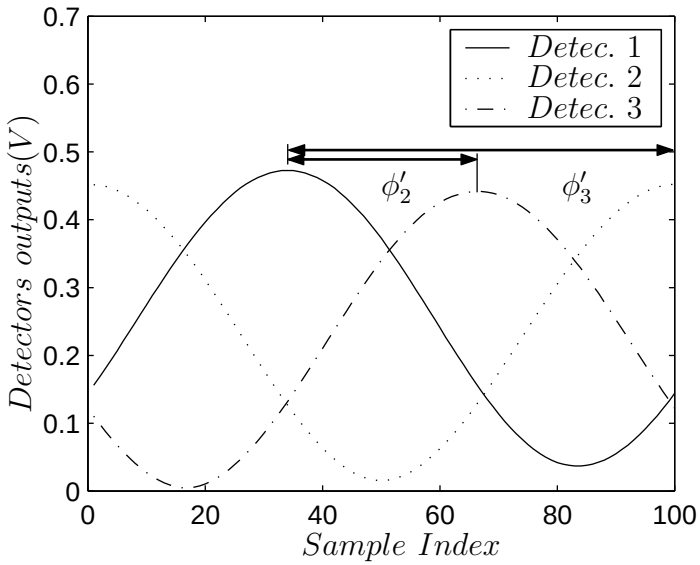

Fig. 3. Voltage measured at the power detectors' outputs

In order to calculate $\hat{v_i}(n)$ from the sampled voltages $v_i(n)$, the values of $a_i V_{LO}^2$ must be found. This is easily executed by making $v_{rf}(t) = 0$ and measuring the detectors' outputs. This is equivalent to connecting a matched load to port 2 of the reflectometer.

The DC terms of (3), $b_i V_{RF}^2(t)$, are obtained by calculating the average values of $\hat{v_i}(n)$, defined as $\overline{\hat{v_i}(n)}$. From these average values, the relationships b_2/b_1 and b_3/b_1 are determined from:

$$\frac{b_i}{b_1} = \frac{\overline{\hat{v_i}(n)}}{\overline{\hat{v_1}(n)}} \quad i = 2, 3 \tag{15}$$

From the sampled voltages, it is also possible to determine $2c_i V_{RF}(n)$ by finding the extreme values of $\hat{v_i}(n)$ and subtracting the maximum point from the minimum value. This allows the calculation of c_2/c_1 and c_3/c_1 as follows:

$$\frac{c_i}{c_1} = \frac{max(\hat{v_i}(n)) - min(\hat{v_i}(n))}{max(\hat{v_1}(n)) - min(\hat{v_1}(n))} \quad i = 2, 3 \tag{16}$$

 ISSN 1516-7399

Reminding that we imposed $\phi'_1 = 0$, we finally determine the values of ϕ'_2 and ϕ'_3 using the following expression:

$$\phi'_i = (n_{max}(i) - n_{max}(1))\frac{2\pi}{N} \quad i = 2, 3 \tag{17}$$

where $n_{max}(i)$ are the sample indexes where the maximum values of $\hat{v_i}(n)$ are located.

After obtaining all relative constants, the remaining c_1 and ϕ_0 must be encountered. Expressions (4), (5), (13) and (14) are used for achieving this goal. For applications such as demodulators, where neither absolute amplitude nor absolute phase are necessary, normalization values may be arbitrarily attributed to c_1 and ϕ_0. We may choose $c_1 = 1$ and $\phi_0 = 0$, for instance. If only the amplitude of the incoming signal must be absolutely determined, c_1 may be found by connecting a signal with known constant amplitude at port 2 and acquiring one sample voltage at the output of each power detector. The value of ϕ_0 may be chosen 0. However, if knowing the absolute phase is also important, c_1 and ϕ_0 are found by making at least two voltage measures at each detector output when a known amplitude and frequency signal incomes at port 2.

The final objective of the procedure described above is to determine the coefficients of a linear combination of $v_i(t)$ which is related to the complex envelope $\rho(n)$ of the RF signal incoming at the reflectometer port 2. This relationship is defined as follows:

$$\rho(n) = U(n) + jV(n) = av_1(n) + bv_2(n) + cv_3(n) + d \tag{18}$$

where the constants a, b, c and d are given by:

$$a = (x_1 \cos\phi_0 + y_1 \sin\phi_0) + j(y_1 \cos\phi_0 - x_1 \sin\phi_0) \tag{19}$$

$$b = (x_2 \cos\phi_0 + y_2 \sin\phi_0) + j(y_2 \cos\phi_0 - x_2 \sin\phi_0) \tag{20}$$

$$c = (x_3 \cos\phi_0 + y_3 \sin\phi_0) + j(y_3 \cos\phi_0 - x_3 \sin\phi_0) \tag{21}$$

$$d = -[a(a_1 V_{LO}^2) + b(a_2 V_{LO}^2) + c(a_3 V_{LO}^2)] \tag{22}$$

Wireless receivers containing a five-port discriminator and a local oscillator with frequency f_{LO} may be automatically calibrated following the procedure above. In a manufacturing site, the calibration constants can be found by injecting an RF signal and activating a software service routine which implements the method presented. Then, the constants are recorded in a non-volatile memory for posterior use

IV. Simulation and measurement

We verified the validity of the method by simulating the system of Figure 1 in the ADS-Agilent® enviroment. The five-port reflectometer was designed to operate at 2 GHz . The resolution of the A/D converters was of 12 bits and their dynamics of ± 1 V. 14-bit look-up tables were used to fit the detectors' output voltages into normalized power values [13] in order to extend the validity of (2). We connected a signal generator at port 1 with power and frequency set at 0 dBm and 2 GHz respectively whereas the RF generator connected at port 2 was set at -3 dBm and 2.000001 GHz respectively. Using the *circut envelop* simulation method with *tstep*=10 μs and *tstop*=1 ms, the system was simulated and the voltages at the output detectors were saved in a file for posterior processing. We replaced the RF generator by a 50 Ω load and repeated the previous steps. Other simulations were conducted with the power of the RF generator set at -10 dBm and -20 dBm in order to verify the calibration constants.

In addition to simulations, an experiment was set up as illustrated in Figure 4. It comprises a five-port interferometer implemented in microstrip technology [14] (with different

 ISSN 1516-7399

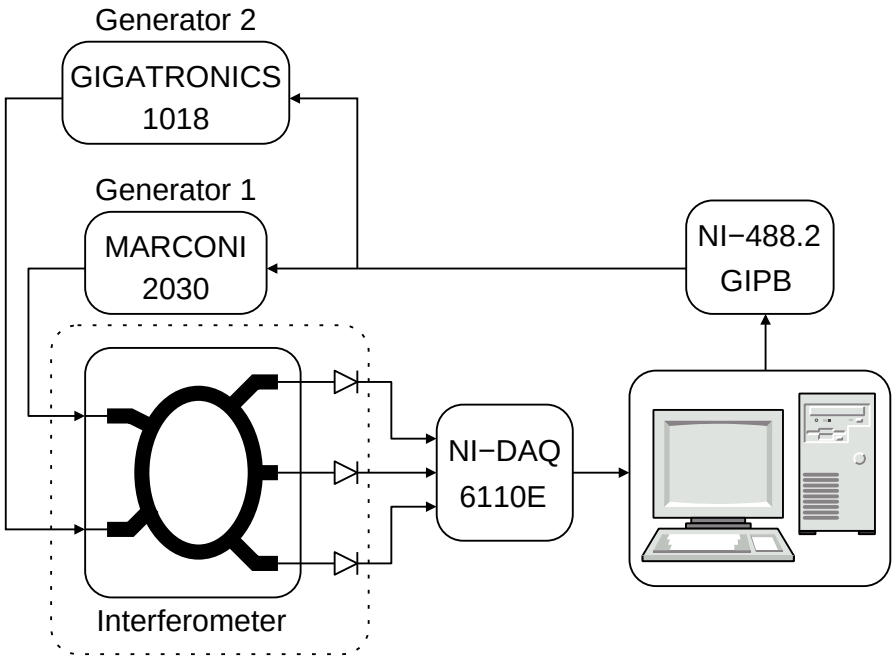

Fig. 4. Five-port arrangement used for measurements

characteristics from the interferometer used in simulations), an RF generator to serve as phase reference (Marconi 2003), a second generator to serve as test signal (Gigatronics 1018), an acquisition board (4 x 12-bit) PCI-6110E from National Instruments® and a microcomputer equipped with a GPIB bus controller

The signal generators were remotely programmed to operate in the same conditions (power and frequency) as they were set for simulations. The acquisition board was set to acquire 100 points with sampling frequency of 100 kHz. The matched load was emulated by setting off the RF generator connected at port 2. The measured voltages were fi t into normalized power values by means of 14-bit look-up tables. Then, the complex ratios between the input signals were calculated using MATLAB scripts. Further processing of the simulated and measured data is detailed in next section.

V. RESULTS

From the data fi les created during simulations and measurements, we performed the calibration procedure using MATLAB® scripts. The values of ϕ_i are obtained by observing the phase shift between the three outputs (Figure 3) as the procedure enumerated in section III indicates.

The calibration constants of the simulated and built reflectometers are summarized in table I. The differences observed between the two sets of constants are expected since the reflectometer designs are different. For both cases, we chose $\phi_0 = 0$ and c_1 was found considering -3 dBm as the reference power. The applications we have been dealing with do not demand absolute phase values.

The evaluation of the achieved calibration was done using voltage values obtained after setting the power of the RF generator at -10 dBm and -20 dBm. The calculated values of $\rho(n)$ are plotted in Figure 5. As the frequency difference between the two input signals was of 1 kHz, the sampling frequency was of 100 kHz and the acquistion time was 1 ms, we notice in the Figure 5 increasing-phase and constant-magnitude complex values for both conditions.

Better insight of the results can be achieved if we show the $\rho(n)$'s magnitude and phase in separate graphics. We notice from Figure 6 the variation of the absolute value as function of

 ISSN 1516-7399

TABLE I

CALIBRATION CONSTANTS FROM SIMULATION AND MEASUREMENT

	Simulation		Measurement	
	Magnitude	Phase (^{o})	Magnitude	Phase (^{o})
a	3.41	-1.88	1.31	-41.72
b	3.01	-114.42	3.40	90.09
c	2.80	116.37	1.62	-137.54
d	0.31	159.34	0.13	-53.24

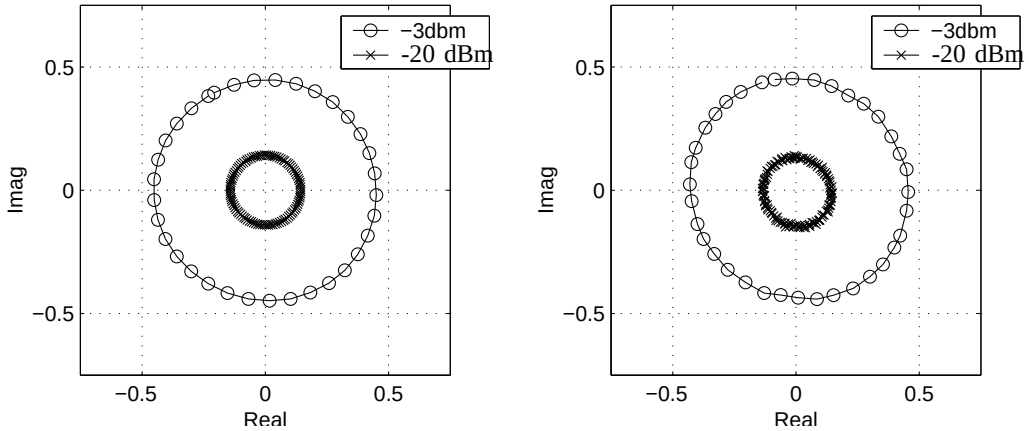

(a) Simulation (b) Measurement

Fig. 5. Complex representation of the calculated values of $\rho(n)$ using simulation and measurement data

the time. The expected values are 0.446 and 0.141 when the RF generator is set to -10 dBm and -20 dBm respectively. In table II a summary of the obtained values is presented. The stronger deviations exhibited by the measures are due to the noisy environment where the experiment was performed as well as to the measurement errors introduced by the instruments.

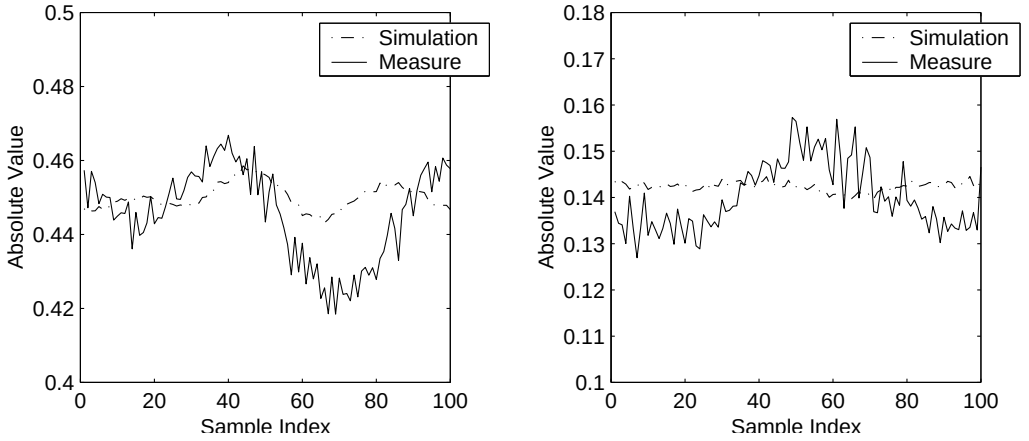

(a) Pin=-10 dBm (b) Pin=-20 dBm

Fig. 6. Absolute Values of $\rho(n)$

The phase of $\rho(n)$ is plotted in Figure 7 where we observe a phase shift between the measurement and the simulation values. This is due to the arbitrary phases of the RF signals

TABLE II

MEAN AND STANDARD DEVIATION OF THE ABSOLUTE VALUES OF $\rho(n)$ CALCULATED FROM SIMULATION AND MEASUREMENT DATA

	Simulation		Measurement	
	Mean	σ	Mean	σ
-10 dBm	0.45	$3.47\text{x}10^{-3}$	0.45	$1.242\text{x}10^{-2}$
-20 dBm	0.14	$9.94\text{x}10^{-4}$	0.14	$7.32\text{x}10^{-3}$

when the acquisitions started. The linear behavior observed proves the effi ciency of the proposed calibration method.

We calculated the derivative of the simulated and measured phase of $\rho(n)$ and sketched them in Figure 8. The derivative eliminates the phase shift between the measurement and the simulation, providing for a better insight of the results.

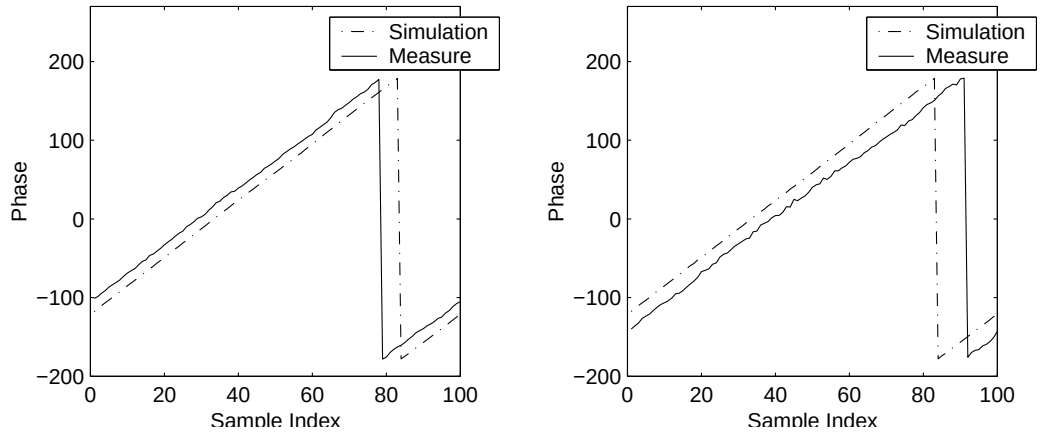

(a) Pin=-10 dBm (b) Pin=-20 dBm

Fig. 7. Phase Values of $\rho(n)$

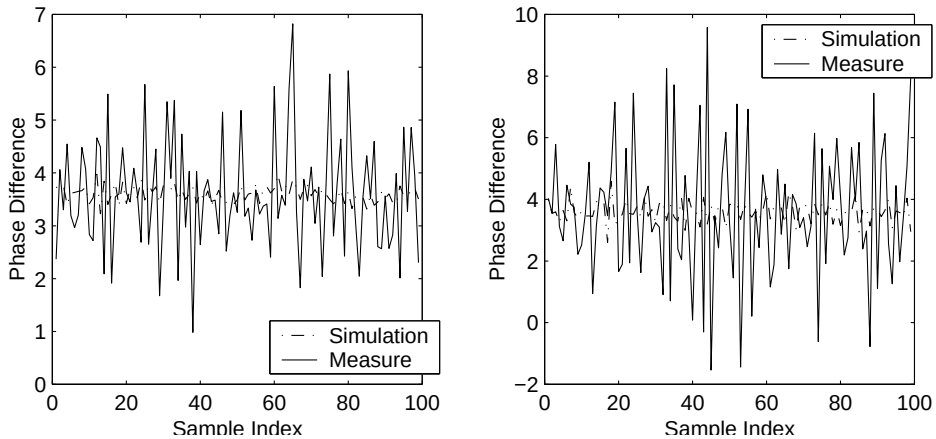

(a) Pin=-10 dBm (b) Pin=-20 dBm

Fig. 8. Derivative of the $\rho(n)$ values

 ISSN 1516-7399

The statistical analysis of these data is presented in table III. As 100 points were acquired during a period of signal, the mean phase difference expected is 3.6°. The deviations σ from the expected value observed are also due to the noisy environment where the experiment was performed and to the measurement errors introduced by the instruments.

TABLE III

MEAN AND STANDARD DEVIATION OF THE PHASE DIFFERENCE BETWEEN CONSECUTIVE SAMPLES OF $\rho(n)$ CALCULATED FROM SIMULATION AND MEASUREMENT DATA

	Simulation		Measurement	
	Mean (°)	σ (°)	Mean(°)	σ (°)
-10 dBm	3.60	0.149	3.59	1.066
-20 dBm	3.60	0.339	3.60	2.166

VI. DISCUSSION OF RESULTS

The results presented in the previous section show that the proposed calibration method is valid. Since the power of the RF generator was set to -3 dBm during the calibration procedure, there are no constraints regarding strong signals as there are in the work of [11]. In their method, a complex offset is added to the value of $\rho(n)$ as the power of the RF signal increases beyond the established conditions. The measures we made setting the RF generator at -10 dBm and at -20 dBm show that the $\rho(n)$ circles are concentrics, meaning that there are no complex offsets incorporated to the expected value.

The standard deviation of the phase difference and the absolute values increased as the power of RF generator decreased. This fact is not due to the calibration constants, though it is caused by environment and quantization noise [15].

VII. CONCLUSION

Five-port systems have been employed as complex signal discriminators in moderns applications. Direct conversion receivers, radars and phase-locked loops are some examples of systems which have used 5-port discriminators. There are a few architectures capable of implementing them. Some of these architectures demand a calibration procedure to determine the reflectometer intrinsic parameters. Most of the calibration procedures found in literature were developed by researchers from the instrumentation and measurement area. We presented in this paper a new method for calibrating five-port reflectometers. The highlights of this procedure are its simplicity and its automatic capability. For instance, a wireless receiver containing a five-port demodulator can be calibrated during manufacturing using an RF signal generator and a software service routine integrated to the proper receiver.

The method was developed from an analytical description of the system which was described in detail in the paper body. To validate the proposal, simulation and measurements were done. The reflectometers used in simulation and measurement had different characteristics as we could identify from the calibration constants encountered. However, the results obtained from test signals were similar and very close to the expected values, certifying the calibration constants and consequently the method.

Although our method in based on a five-port reflectometer, it can be easily adapted for six-port systems. A possible improvement we foresee is the implementation of the proposed procedure in an adaptive environment.

ACKNOWLEDGMENTS

The authors would like to thank CAPES (Coordenação de aprefeiçoamento de pessoal de nível superior) and COFECUB (Comité Français d'Evaluation de la Coopération Universitaire avec le Brésil) for the award of fellowships during the period of this work.

 ISSN 1516-7399

REFERENCES

[1] G. F. Engen, "The six-port reflectometer: An alternative network analyzer," *IEEE Transactions on Microwave Theory and Techniques*, vol. 25, no. 12, pp. 1075–1080, December 1977.

[2] S. O. Tatu, E. Moldovan, K. Wu, and R. G. Bosisio, "A new direct millimeter-wave six-port receiver," *IEEE Transactions on microwave theory and techniques*, vol. 49, no. 12, pp. 2517–2522, December 2001.

[3] A. A. Abidi, "Direct-conversion radio transceivers for digital communications," *IEEE Journal of solid-state circuits*, vol. 30, no. 12, december 1995.

[4] J. Hyyrylainen and L. Bogod, "Six-port direction conversion receiver," in *Proceedings of the 27th microwave conference and exhibition*, 1997, pp. 341–346.

[5] G. Neveux, B. Huyart, and J. R. Guisantes, "Rf demodulator with a "six-port"system," in *Proceedings of 31nd European Microwave Conference*, 2001.

[6] M. Ratni, D. Krupezevic, V. Brankovic, M. Abe, and N. Sasho, "Design considerations for direct conversion receiver using five-port circuit," in *Proceedings of 31nd European Microwave Conference*, 2001.

[7] C. G. Migélez, B. Huyart, E. Bergeault, and L. P. Jallet, "A new automobile radar based on the six-port phase/frequency discriminator," *IEEE Transactions on vehicular technology*, vol. 49, no. 4, pp. 1416–1423, July 2000.

[8] F. R. de Sousa and B. Huyart, "A reconfigurable phase-locked loop," in *To appear in IEEE Instrumentation and Measurement Conference Proceedings*, may 2003.

[9] F. Wiedman, B. Huyart, E. Bergeault, and L. Jallet, "A new robust method for six-port reflectometer calibration," *IEEE Transactions on Instrumentation and Measurements*, vol. 48, pp. 927–931, 1999.

[10] Y. Liu, "Calibrating an industrial microwave six-port instrument using the artificial neural network technique," *IEEE Transactions on Instrumentation and Measurements*, vol. 45, no. 2, pp. 651–656, 1996.

[11] G. Neveux, B. Huyart, and J. Rodriguez, "Auto-calibrage d'un demodulateur utilisant la technique five-port"," in *To appear in: 13émes Journées Nationales Microondes*, may 2003.

[12] C. Potter and A. Bullock, "Non linearity correction of microwave diode detectors using a repeatable attenuation step," *Microwave Journal*, vol. 36, pp. 272,274,277–279, May 1983.

[13] F. R. Sousa, G. Neveux, B. G. Amante, and B. Huyart, "Five port junction: In the way of general public applications," in *Proceedings of 32nd European Microwave Conference*, 2002.

[14] F. Sousa, B. Huyart, and R. Freire, "Low cost network analyser using a six-port," in *Proceedings of 2001 International Microwave and Optoelectronics Conference - IMOC 2001*, 2001.

[15] F. R. Sousa, B. Huyart, and R. N. de Lima, "Avaliação dos efeitos de quantização em sistemas baseados em reflect ômetros de cinco portas," in *Proceedings of X Simpósio Brasileiro de Microondas e Optoeletrônica*, 2002, pp. 61–65.

 ISSN 1516-7399